Particle-in-Cell Simulation Studies for Hybrid Laser-Plasma Accelerators and Plasma Eyepieces

M. Zeng, A. Martinez de la Ossa, J. Osterhoff

published in

NIC Symposium 2020
M. Müller, K. Binder, A. Trautmann (Editors)

Forschungszentrum Jülich GmbH,
John von Neumann Institute for Computing (NIC),
Schriften des Forschungszentrums Jülich, NIC Series, Vol. 50,
ISBN 978-3-95806-443-0, pp. 415.
http://hdl.handle.net/2128/24435

Particle-in-Cell Simulation Studies for Hybrid Laser-Plasma Accelerators and Plasma Eyepieces

Ming Zeng, Alberto Martinez de la Ossa, and Jens Osterhoff

Deutsches Elektronen-Synchrotron DESY, 22607 Hamburg, Germany
E-mail: jens.osterhoff@desy.de

Plasma wakefield accelerators driven by either laser or electron beams have shown great potential for future applications. Output beam quality from plasma has improved tremendously over the past decade. This, to a large extend, was enabled by progress in high-performance computing and numerical techniques based on particle-in-cell simulations. In this proceedings paper, we present two recent simulation studies, on hybrid plasma accelerators and on plasma-based laser focusing, opening new avenues in the application of compact accelerators and for the generation of high-brightness electron beams.

1 Introduction

Laser-driven (LWFAs)[1] and beam-driven (PWFAs) plasma wakefield accelerators[2] can generate accelerating electric fields of 10 to 100 GV/m, many orders of magnitude higher than achievable with conventional radio frequency (RF) technology. This enables a path towards greatly miniaturised and, therefore, cost-effective particle accelerators with a significant societal impact potential. Such a development may allow for the proliferation of high-energy accelerator technology far beyond national-lab-scale research centres and could multiply access opportunities to, for example, accelerator-based cutting-edge photon science machines such as free electron lasers. Furthermore, it will notably lower the financial entrance bar for developing countries to engage in accelerator research.

Great progress over the past decades has led to the successful demonstration of GeV-range beams accelerated on only centimetre scales in plasma[3] and improved control and stability.[4] However, achieving the required beam quality for the envisioned disruptive application of novel accelerators in photon science, material science, medicine, and particle physics remains a challenge. Due to the micrometre spatial scale and femtosecond duration of the acceleration structure, the experimental diagnostics and optimisation of LWFAs and PWFAs are challenging. Thus, computer simulation algorithms, in particular Particle-in-Cell (PIC) techniques, have proven successful and are a cornerstone of predictive plasma accelerator research.[5, 6]

In PIC algorithms, fields (electric force, magnetic force, currents, *etc.*) are deposited onto grids (or cells) while particles are modelled as clouds (or shaped macro-particles) with the volume of one or a few adjacent cells. One macro-particle commonly contains a large number of real particles such that the number of particles for computation purposes is largely reduced. Time steps in PIC are chosen such that charged macro particles and fields only propagate to nearby cells making massive parallelisation possible.

In this proceeding, we demonstrate progress in our simulation studies of laser and plasma wakefield accelerators. In Sec. 2 we show a pioneering study on hybrid Laser-Plasma Accelerators (LPWFA), which deploy an LWFA-generated electron beam to drive

a PWFA stage. In Sec. 3 we present our concept of a laser-plasma telescope system with a plasma eyepiece to flexibly adjust the laser spot sizes.

2 Simulation Studies on Hybrid Laser-Plasma Accelerators

2.1 Motivation

PWFAs are considered to offer improved control over the process of injection and acceleration of a witness beam compared to LWFAs. One of the reasons lies in the way that electron-beam drivers propagate through plasma, being immune to the dephasing and diffraction effects affecting the performance of LWFAs. Thus, in principle, PWFAs may allow for longer and more stable acceleration lengths, resulting in higher energy and potentially higher quality beams. However, a major limitation for the widespread use of PWFA technology is the requirement of a large-scale accelerator facility providing the drive beams. In contrast, with a comparably compact size, high-power laser facilities for LWFAs have proliferated over the past decade and electron beams with several hundreds of picocoulomb charge are nowadays routinely generated by LWFAs.[7, 8] In a hybrid LWFA-driven PWFA (LPWFA), the LWFA-generated high-current electron beam is used as driver

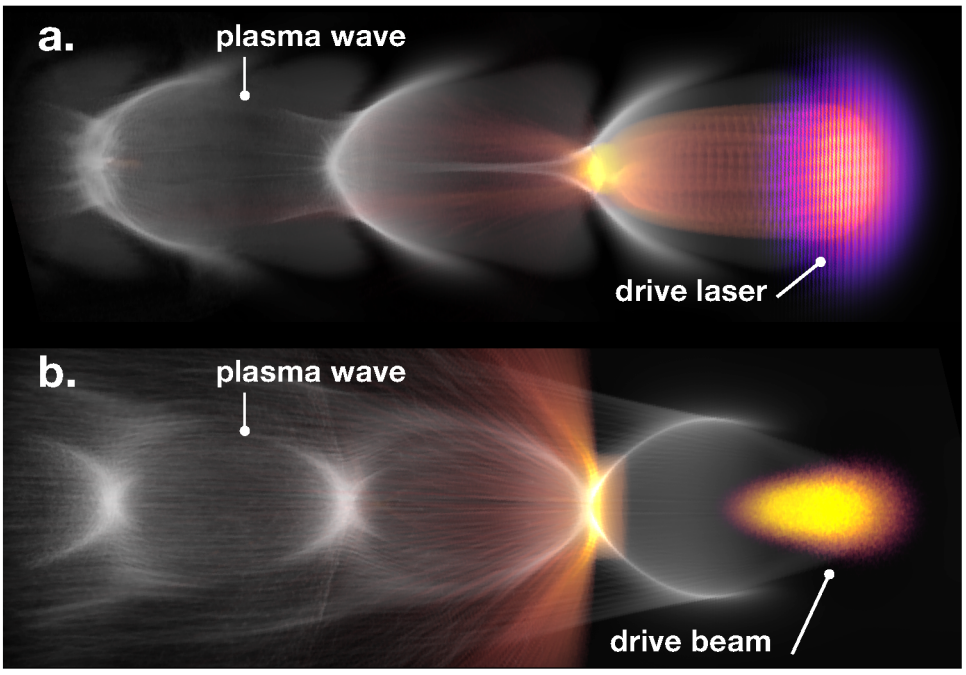

Figure 1. OSIRIS PIC simulations for an LWFA (**a.**) and a PWFA (**b.**). The figures show a laser and electron-beam driving a plasma-electron density wave. The density of electrons being injected is also shown. In both simulations injection is triggered by means of induced ionisation. In a hybrid Laser-Plasma Accelerator (LPWFA) both plasma acceleration principles are combined for the production of superior quality beams from a particularly compact setup.

of a subsequent PWFA stage. In the PWFA stage, a new witness beam with largely improved quality is to be generated and accelerated to higher energies.[9–12] In essence, the PWFA stage operates as a beam brightness and energy transformer of the LWFA output, aiming to reach the demanding beam quality requirements of *e. g.* a free-electron laser (FEL), without sacrificing the small spatial footprint and the relatively low cost offered by LWFAs.

2.2 PIC Simulations for Conceptual Design

In order to assess the feasibility of the hybrid LPWFA concept, detailed 3D PIC simulations were performed with the code OSIRIS[13] for the LWFA and PWFA stages. As illustrated in Fig. 1, the OSIRIS code is capable to reproduce with high fidelity the physics of the process of injection and acceleration of witness beams for both kind of plasma accelerators. Supported by large-scale PIC simulations performed on the JUWELS supercomputer at JSC, a conceptual study for hybrid LPWFAs acting as energy and brightness transformers was recently published.[14] Our results highlight that, by utilising electron beams produced in current LWFA laboratories as drivers of a PWFA, a new generation of ultrashort (femtosecond), high-energy and high-brightness electron beams could be produced. The improvement with respect to the original LWFA beam can be a factor two in energy and about a factor 100 000 in brightness, potentially enabling beam-quality demanding applications such as future compact FELs.

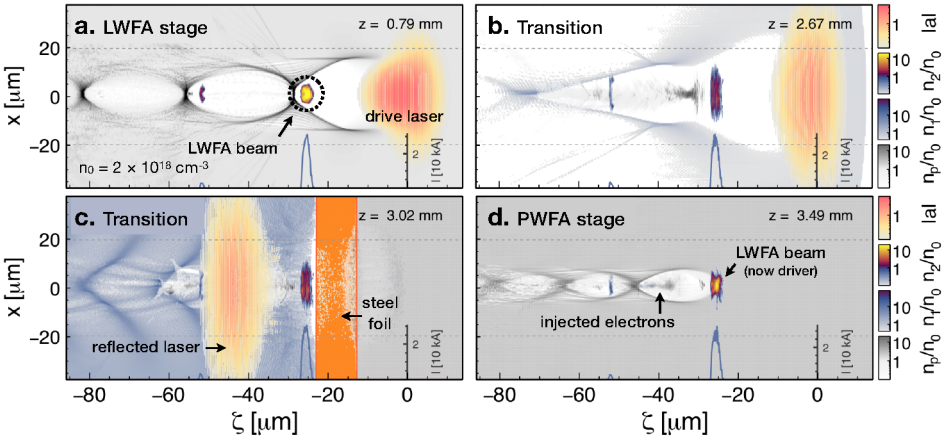

Figure 2. Start-to-end simulation demonstrating the feasibility of a LWFA-to-PWFA transition in the hybrid LPWFA experiment at HZDR. The process is initiated with a laser driving a plasma accelerator in a first gas jet and producing a high-current electron beam (**a.**). Both the laser and the produced beam exit the first stage and enter a second gas jet (**b.**). A 12.5 μm thin steel foil is placed in the beginning of the second jet to reflect the laser, while letting the electron beams go through (**c.**). With the laser removed from second stage, the LWFA-created beam drives a plasma accelerator in which background electrons may be trapped and form a new higher quality witness beam (**d.**).

2.3 PIC Simulations for Proof-of-Concept Experiment

Motivated by the promising simulations results shown in Ref. 14, we have explored the feasibility of this concept through dedicated experiments at Helmholtz-Zentrum Dresden-Rossendorf (HZDR),[15] using the DRACO laser system[16] for the LWFA stage and the thereby produced electron beam as driver for a subsequent PWFA stage. First experimental results are outstanding, demonstrating for the first time that LWFA beams can drive a high-gradient PWFA by themselves at a high plasma density ($\sim 4 \times 10^{18}$ cm^{-3}), where accelerating gradients surpassing 100 GV/m are expected. In conjunction with the direct observation of beam-driven plasma waves, evidence of the acceleration of a new witness beam in the PWFA stage has been observed. Dedicated PIC simulations reproducing the concatenation of both stages have been performed, exhibiting a remarkable qualitative similarity with the experiments, and demonstrating accelerating gradients higher than 100 GV/m in the dedicated PWFA stage. This kind of start-to-end simulations (*c.f.* Fig. 2), performed on JUWELS at JSC, represent a milestone by themselves as they address for the first time key aspects of the LWFA-to-PWFA transition process.

An article containing full details is being reviewed for publication.[17]

3 Simulation Studies on Plasma Eyepieces for Petawatt-Class LWFAs

3.1 Motivation

Nowadays petawatt lasers have become high-priority tools for studying the intrinsic properties of the microscopic physical world.[18] Manipulation of such powerful lasers is a big challenge due to the lack of high damage-threshold optical materials. The current solution is to use large beam apertures so that the laser power is spread across a large area of the optical element to prevent damage. As a consequence the diameter of the final focusing mirror needs to be of the order of a considerable fraction of a metre to prevent breakdown of the optic. This leads to the focusing system being costly and difficult to replace. One has to prepare a few focusing systems with different focal lengths for different applications, which makes the difficulty more intractable. For LWFA applications usually a fixed moderately relativistic laser intensity of the order of 10^{18} $\mathrm{W/cm}^{-3}$ at focus is required, which means increasing focal spot sizes and focal lengths with the increasing laser power. This may lead to extremely long focal lengths of the order of 100 (1000) metres for future 10 (100) petawatt lasers.

We have introduced a telescope system to solve these difficulties.[19] As illustrated in Fig. 3, a laser beam is pre-focused by conventional optics with the focal length of f_0 to position z_0 in vacuum with the waist radius of w_0 and normalised peak vector potential amplitude of $a_{0\mathrm{peak}}$. Then it propagates in vacuum for a distance d and touches the vacuum-plasma interface at z_1. Afterwards the laser undergoes self-focusing[20] and is refocused at z_2 with the spot size radius of w_2 and normalised peak vector potential amplitude of $a_{2\mathrm{peak}}$, where w_2 is the first local maximum of laser spot size radius in the plasma. The thickness of the plasma required $l = z_2 - z_1$ is referred to as the thickness of the plasma eyepiece. Finally, the total function of this setup is to focus the laser beam to an effective spot size of w_2 within a distance of $f = f_0 + d + l$. Due to the strong plasma response to the laser beam, d and l are usually much smaller than f_0 so that $f \approx f_0$. Thus, the advantage of such a setup is obvious: a conventional focusing optic for reaching the focal spot

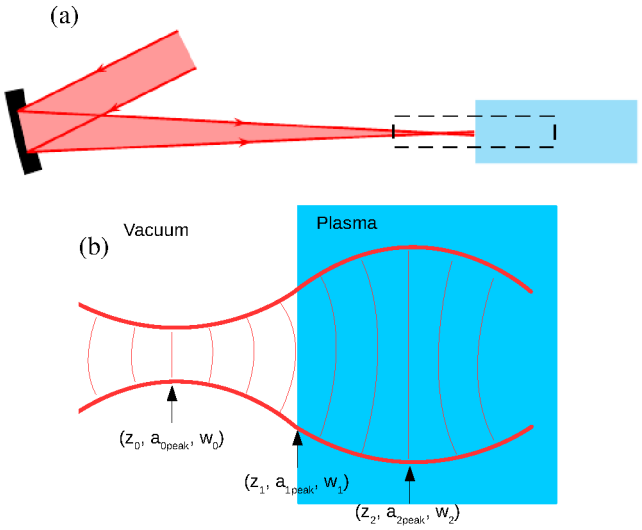

Figure 3. Schematic view of the laser profile (thicker red curves) evolution in the plasma eyepiece region. The laser is pre-focused in vacuum by conventional optics as shown in (a), with the dashed box region shown in (b). The focal plane is at z_0 and laser peak normalised vector potential amplitude is $a_{0\mathrm{peak}}$ and spot size is w_0. After a distance $d = z_1 - z_0$ the laser enters the plasma region start at z_1. Due to the self-focusing effect of lasers in plasmas, the laser wavefront (thinner red curves) is bent concavely and becomes flat again at z_2. As a consequence the laser spot size reaches a local maximum of w_2.

size of w_2 would have the focal length of fw_2/w_1 which can be several times longer than our setup. Moreover, one can easily adjust the effective focal spot size w_2 by changing the plasma density and d with the telescope system, while in a conventional focusing system one has to replace the large and expensive focal optics for different focal spot sizes.

We show one simulation example performed by OSIRIS[13] in Fig. 4. The simulation is initialised ($t = 0$) at around $z_1 = 0$ with the laser focal plane at $k_p z_0 = -60$, where $k_p = \sqrt{4\pi r_e n_p}$ is the plasma wave number, n_p is the background plasma density and $r_e \approx 2.82 \times 10^{-15}$ m is the classical electron radius. The laser focal waist radius is $k_p w_0 = 4$, thus the laser spot size at the vacuum-plasma interface is $k_p w_1 = 5$. The simulation grid information is the same as the simulations shown in Sec. 3.2. After propagating a distance $k_p l = 76$ ($\omega_p t = 76$), the laser spot size reaches a local maximum of $k_p w_2 = 6.2$ due to self-focusing effect.

3.2 Scan of a 4-Dimensional Parameter Space

We have done an analytical study of the plasma eyepiece which is based on non-perturbed plasma assumptions.[19] In the blowout regime the ponderomotive force of the laser is so strong that almost all of the plasma electrons are driven out of the laser axial region,[21,22] thus the non-perturbed plasma model reaches its limits and PIC simulations are required.

We have performed full 3-dimensional PIC simulations on JUWELS using the code OSIRIS[13] to scan the 4-dimensional parameter space (k/k_p, $k_p w_0$, $a_{0\mathrm{peak}}$, $k_p d$). The longitudinal simulation box size is $10k_p^{-1}$, and the lengths of the two transverse dimensions

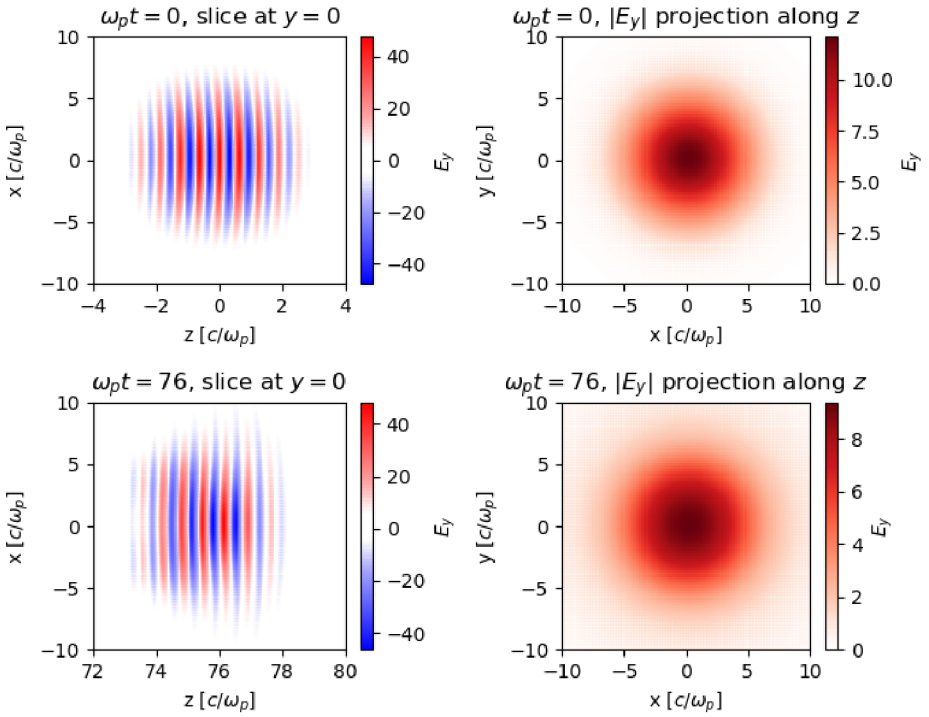

Figure 4. An example simulation of the laser evolution in the plasma eyepiece region. The parameters are $k/k_p = 10$, $k_p w_0 = 4$, $k_p d = 60$, $a_{0\mathrm{peak}} = 10$ and laser FWHM duration is $\omega_p \tau = 4$. The plasma region starts at $z_1 = 0$ and is half-infinitely long. The simulation started at the vacuum-plasma interface $z_1 = 0$ at $t = 0$ (top two subplots). At $k_p z_2 = 76$ (bottom two subplots) the laser spot size reaches a local maximum of $k_p w_2 \approx 6.2$. The left column subplots are the slices of the laser electric field side view, and the right column subplots are the projections of the absolute value of the laser electric field to the x-y plane (front view).

k/k_p	Low resolution	High resolution
10	256×256^2	512×512^2
20	512×256^2	1024×512^2
30	512×256^2	1024×512^2
40	1024×256^2	2048×512^2

Table 1. Longitudinal and transverse number of cells used for different values of k/k_p in the simulations. Two resolutions are used to confirm the convergence of the simulations.

are taken as 10 times of the estimated value of w_2 (to be discussed below). Two resolutions have been adopted to confirm the convergence of the simulations according to Tab. 1, while the higher resolution results are taken as the final results. The full-width-at-half-maximum (FWHM) laser pulse duration is fixed as $\omega\tau_{\mathrm{FWHM}} = 4$. The simulations are initialised at $t = 0$ with laser centre at $z = z_1 = 0$, while the laser focal planes are at $-k_p d$.

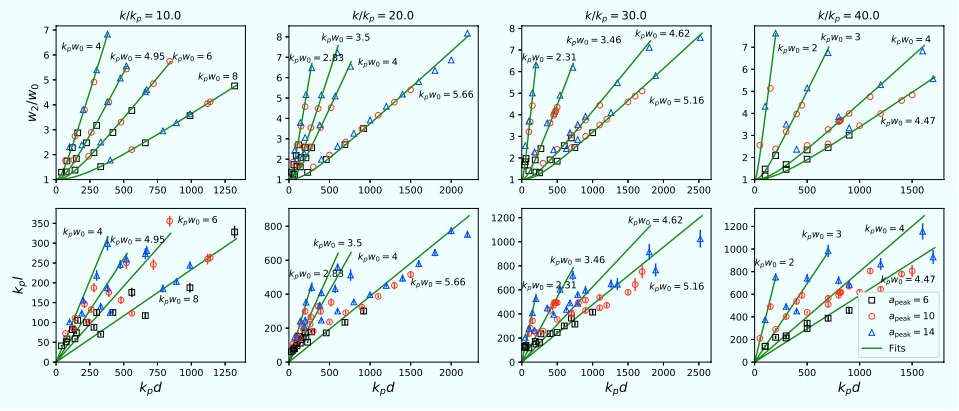

Figure 5. Simulation results for w_2/w_0 (row 1) and l (row 2) *vs.* d for different laser and plasma parameters (k/k_p, k_pw_0, $a_{0\mathrm{peak}}$). In each subplot, the results for $a_{0\mathrm{peak}} = 6$, 10 and 14 are marked as black squares, red circles and blue triangles, respectively. The green lines are the fits of the data with the same k/k_p and k_pw_0 by Eq. 1, with k_pw_0 near the green lines. The laser wave number parameter normalised to the plasma wave number k/k_p takes the values 10, 20, 30 and 40 as shown on the top of each column.

In each diagnostic point of the simulations, the absolute value of the laser electric field is projected to the $x-y$ plane (front-view), and two-dimensional Gaussian fit (with the function $E = E_0 \exp\left[-(x-x_0)^2/w^2 - (y-y_0)^2/w^2\right]$) is performed for the laser radius w. The values of w_2 are measured by taking the local maximum of w *vs.* z and the values of plasma eyepiece thickness $l = z_2 - z_1$, where z_2 is the location of the local maximum of w.

Simulation results for w_2 and l are collected and plotted in Fig. 5. We have found that w_2 can be estimated by a function

$$\frac{w_2}{w_0} = \sqrt{1 + \frac{d^2}{\zeta^2}} \tag{1}$$

where

$$k_p\zeta \approx (0.950 - 0.0027k/k_p)k_pz_R - 1.17k/k_p - 12.6 \tag{2}$$

From Fig. 5 we have also found l almost linear depends on d, *i. e.*

$$l = \chi d \tag{3}$$

where

$$\chi \approx 21.0\,(k_pw_0)^{-2.08} \tag{4}$$

Eqs. 1-4 predict excellent scalability of the telescope system including a plasma eyepiece. In a petawatt-class laser system one can largely reduce the space required for the focus system. We show two exemplary simulations in Fig. 6.

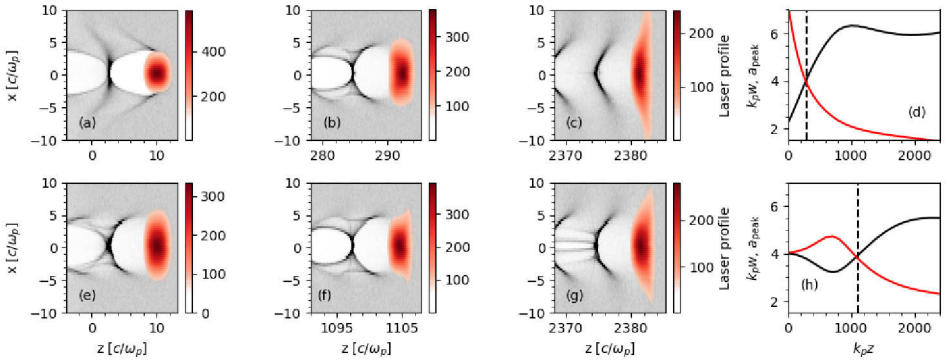

Figure 6. Comparative simulations with (a to d) and without (e to h) a plasma eyepiece. The effective laser spot size adjusted by the plasma eyepiece in (a) - (d) is approximately the laser spot size in the later case, but the former case has a much reduced focal length of the pre-focusing conventional optics system.

4 Conclusion

We have demonstrated two schemes towards future laser and plasma wakefield accelerators. The first is the hybrid laser-plasma wakefield accelerator, which largely reduces the setup scale of a conventional PWFA and promises the possibility to perform PWFA studies in a small size laser laboratory. The second is the laser-plasma telescope system using a plasma eyepiece, which largely reduces the focal space required in a LWFA driven by a petawatt-class laser, and enables the scan of laser spot size parameters. Our studies using large-scale parallelled PIC simulations demonstrate the potential of supercomputing for calculating complex systems such as laser-plasmas.

Acknowledgements

We thank the OSIRIS consortium (IST/UCLA) for access to the OSIRIS code. We also gratefully acknowledge the Gauss Centre for Supercomputing e.V. (`www.gauss-centre.eu`) for funding this project by providing computing time through the John von Neumann Institute for Computing (NIC) on the GCS Supercomputer JUWELS at Jülich Supercomputing Centre (JSC). This work is supported by the Helmholtz MT ARD scheme and the Helmholtz ZT-0009 project.

References

1. T. Tajima and J. M. Dawson, *Laser Electron Accelerator*, Phys. Rev. Lett. **43**, 267–270, 1979.
2. P. Chen, J. M. Dawson, R. W. Huff, and T. Katsouleas, *Acceleration of Electrons by the Interaction of a Bunched Electron Beam with a Plasma*, Phys. Rev. Lett. **54**, 693–696, 1985.

3. W. P. Leemans, B. Nagler, A. J. Gonsalves, Cs. Tóth, K. Nakamura, C. G. R. Geddes, E. Esarey, C. B. Schroeder, and S. M. Hooker, *GeV electron beams from a centimetre-scale accelerator*, Nat. Phys. **2**, 696, 2006.
4. J. Osterhoff, A. Popp, Zs. Major, B. Marx, T. P. Rowlands-Rees, M. Fuchs, M. Geissler, R. Hörlein, B. Hidding, S. Becker, E. A. Peralta, U. Schramm, F. Grüner, D. Habs, F. Krausz, S. M. Hooker, and S. Karsch, *Generation of Stable, Low-Divergence Electron Beams by Laser-Wakefield Acceleration in a Steady-State-Flow Gas Cell*, Phys. Rev. Lett. **101**, 085002, 2008.
5. C. K. Birdsall and D. Fuss, *Clouds-in-clouds, clouds-in-cells physics for many-body plasma simulation*, Journal of Computational Physics **3**, 494–511, 1969.
6. J. M. Dawson, *Particle simulation of plasmas*, Rev. Mod. Phys. **55**, 403–447, 1983.
7. J. P. Couperus, R. Pausch, A. Köhler, O. Zarini, J. M. Krämer, M. Garten, A. Huebl, R. Gebhardt, U. Helbig, S. Bock, K. Zeil, A. Debus, M. Bussmann, U. Schramm, and A. Irman, *Demonstration of a beam loaded nanocoulomb-class laser wakefield accelerator*, Nature Communications **8**, 487, 2017.
8. M. Zeng, M. Chen, Z.-M. Sheng, W. B. Mori, and J. Zhang, *Self-truncated ionization injection and consequent monoenergetic electron bunches in laser wakefield acceleration*, Physics of Plasmas **21**, 030701, 2014.
9. B. Hidding, G. Pretzler, J. B. Rosenzweig, T. Königstein, D. Schiller, and D. L. Bruhwiler, *Ultracold Electron Bunch Generation via Plasma Photocathode Emission and Acceleration in a Beam-Driven Plasma Blowout*, Phys. Rev. Lett. **108**, 35001, 2012.
10. A. Martinez de la Ossa, J. Grebenyuk, T. J. Mehrling, L. Schaper, and J. Osterhoff, *High-Quality Electron Beams from Beam-Driven Plasma Accelerators by Wakefield-Induced Ionization Injection*, Phys. Rev. Lett. **111**, 245003, 2013.
11. G. Wittig, O. Karger, A. Knetsch, Y. Xi, A. Deng, J. B. Rosenzweig, D. L. Bruhwiler, J. Smith, G. G. Manahan, Z.-M. Sheng, D. A. Jaroszynski, and B. Hidding, *Optical plasma torch electron bunch generation in plasma wakefield accelerators*, Phys. Rev. ST Accel. Beams **18**, 081304, 2015.
12. A. Martinez de la Ossa, Z. Hu, M. J. V. Streeter, T. J. Mehrling, O. Kononenko, B. Sheeran, and J. Osterhoff, *Optimizing density down-ramp injection for beam-driven plasma wakefield accelerators*, Phys. Rev. Accel. Beams **20**, 091301, 2017.
13. R. A. Fonseca, L. O. Silva, F. S. Tsung, V. K. Decyk, W. Lu, C. Ren, W. B. Mori, S. Deng, S. Lee, T. Katsouleas, and J. C. Adam, *OSIRIS: A Three-Dimensional, Fully Relativistic Particle in Cell Code for Modeling Plasma Based Accelerators*, in Computational Science – ICCS 2002, P. M. A. Sloot, A. G. Hoekstra, C. J. K. Tan, and J. J. Dongarra (Editors), Springer, 342–351, 2002.
14. A. Martinez de la Ossa, R. W. Assmann, M. Bussmann, S. Corde, J. P. Couperus Cabadağ, A. Debus, A. Döpp, A. Ferran Pousa, M. F. Gilljohann, T. Heinemann, B. Hidding, A. Irman, S. Karsch, O. Kononenko, T. Kurz, J. Osterhoff, R. Pausch, S. Schöbel, and U. Schramm, *Hybrid LWFA–PWFA staging as a beam energy and brightness transformer: conceptual design and simulations*, Phil. Trans. R. Soc. A **377**, 20180175, 2019.
15. T. Heinemann, R. W. Assmann, J. P. Couperus, B. Hidding, A. Knetsch, O. Kononenko, A. Köhler, T. Kurz, U. Schramm, O. Zarini, A. Irman, and A. Martinez de la Ossa, *Investigating the Key Parameters of a Staged Laser- and Particle Driven Plasma Wakefield Accelerator Experiment*, in Proceedings of International Particle Accelerator Conference (IPAC '17), 1703–1706, 2017.

16. U. Schramm, M. Bussmann, A. Irman, M. Siebold, K. Zeil, D. Albach, C. Bernert, S. Bock, F. Brack, J. Branco, J. P. Couperus, T. E. Cowan, A. Debus, C. Eisenmann, M. Garten, R. Gebhardt, S. Grams, U. Helbig, A. Huebl, T. Kluge, A. Köhler, J. M. Krämer, S. Kraft, F. Kroll, M. Kuntzsch, U. Lehnert, M. Loeser, J. Metzkes, P. Michel, L. Obst, R. Pausch, M. Rehwald, R. Sauerbrey, H. P. Schlenvoigt, K. Steiniger, and O. Zarini, *First results with the novel petawatt laser acceleration facility in Dresden*, Journal of Physics: Conference Series **874**, 012028, 2017.
17. T. Kurz, T. Heinemann, M. F. Gilljohann, Y. Y. Chang, J. P. Couperus Cabadağ, A. Debus, O. Kononenko, R. Pausch, S. Schöbel, R. W. Assmann, M. Bussmann, H. Ding, J. Götzfried, A. Köhler, G. Raj, S. Schindler, K. Steiniger, O. Zarini, S. Corde, A. Döpp, B. Hidding, S. Karsch, U. Schramm, A. Martinez de la Ossa, and A. Irman, *Demonstration of a compact plasma accelerator powered by laser-accelerated electron beams*, 2019, arXiv:1909.06676 [physics.acc-ph].
18. E. Cartlidge, *Physicists are planning to build lasers so powerful they could rip apart empty space*, Science, 2018, doi:10.1126/science.aat0939.
19. M. Zeng, A. Martinez de la Ossa, K. Poder, and J. Osterhoff, *Plasma Lenses for Relativistic Laser Beams in Laser Wakefield Accelerators*, 2019, arXiv:1901.07974 [physics.plasm-ph].
20. C. E. Max, J. Arons, and A. B. Langdon, *Self-Modulation and Self-Focusing of Electromagnetic Waves in Plasmas*, Phys. Rev. Lett. **33**, 209–212, 1974.
21. A. Pukhov and J. Meyer-ter Vehn, *Laser wake field acceleration: the highly nonlinear broken-wave regime*, Appl. Phys. B **74**, 355–361, 2002.
22. W. Lu, M. Tzoufras, C. Joshi, F. S. Tsung, W. B. Mori, J. Vieira, R. A. Fonseca, and L. O. Silva, *Generating multi-GeV electron bunches using single stage laser wakefield acceleration in a 3D nonlinear regime*, Phys. Rev. ST Accel. Beams **10**, 061301, 2007.